An application of the energy partition method on the blast response of composite panels

T. Li Piani [1], J. Weerheijm [1,2], F. Moriniere [3], J. Hoogland [1],
I. Schipperen [1], G. Roebroeks [1], R. Alderliesten [2]

[1] TNO, The Hague, the Netherlands
[2] TU Delft, Delft University of Technology, Delft, the Netherlands
[3] Ansys, Cambridge, United Kingdom

Landmines are used in battle fields to damage military vehicles. Current vehicle applications in Out of area operations (OoA) are mainly based on steel and aluminum. These offer protection at the expenses of high weight, mobility limitations and design restrictions. A prototype of composite panel which outperforms the blast response of traditional materials was recently developed at TNO, in the Netherlands. In order to address the physics of response, an Energy Partition Method (EPM) has been applied to simulate and interpret the blast behavior of composites experimentally tested. Flexural deformation and delamination were the energy dissipation components implemented in a 1D model of the panel. The results showed that delamination is the first failure mode activated during blast load but its direct contribution on energy dissipation is relatively modest. In contrast, flexural response governs failure against blast load and degradation of the properties of the laminate plies starts after the peak impulse. Interpretation of results showed that aside its modest direct contribution, delamination may trigger the shift from bending to a preferred membrane behavior of the panel, which thus indirectly governs the failure response. In this paper, the EPM adopted framework is described. Experimental and numerical reference consisting of several blast tests and simulations on ¼ panels is briefly recalled. Model implementation and EPM simulation results are presented and interpreted against current knowledge on impact response of composites.

Key words: composite, blast, transient deformation, energy partition method, delamination

1 Introduction

Military vehicles in out of area operations (OoA) are exposed to a wide range of threats, including IED and rifle attacks. The safety of a military vehicle including its occupants is its ability to withstand threats including ballistic impacts of projectiles as well as fragments and blast load of landmines (Berhe, 2007). Materials such as steel and aluminum have been extensively used in protective systems as well as for structural applications in battle fields (Mohotti et al., 2015). These generally provide high levels of protection to the vehicle at the expenses of high specific weight, life cycle costs and end of life dissipation issues. In turn, these may compromise production logistics and vehicle mobility, design flexibility and repair operations feasibility (Alderliesten & Benedictus, 2008). Therefore, protection-effective material solutions for lighter, more agile and durable military vehicles were researched in recent times (Roebroeks, 2017b). Composites have been recently targeted as impact resistant materials in light of their low specific density, durability and relatively life-cycle cheapness (López-Puente et al., 2007). In 2015, a glass fibre composite Laminate (FL) prototype was developed at TNO - DSS, Defence, Safety and Security as a composite solution for vehicle underbelly against mine blasts. This was conceived on the basis of the hypothesis that an early delamination may be effective against blast loadings, because this would trigger the shift from a local bending to a preferred membrane behavior. Experimental programs proved that the mechanical performance of these new composite laminates can outperform traditional aluminum applications on an equal weight basis. This potentially imply a substantial benefit in panel weight for equal blast protection performance with respect to common metallic materials (Roebroeks, 2017b). However, no direct measurements of delamination coalescence and propagation inside the laminate could be definitely gained from experimental setup and research is needed to identify the physics of response and reconstruct the dynamics of blast to panel interaction. To this end, numerical tools are needed (Phu Nguyen et al., 2010). Finite element models have been extensively used to simulate the mechanical behavior of composites (F. Van der Meer et al., 2012). Damage mechanics or plasticity frameworks are generally implemented to address an extended range of material configurations and loading conditions, ranging from fatigue to impact (F. P. van der Meer & Sluys, 2009). FE models are capable of describing the mechanics of material response and the corresponding failure mechanisms with a high degree of details (Li Piani, Weerheijm, & Sluys, 2019). However, this often happens at the expenses of struggling implementation costs and non-obvious material parameters identification practices (Allix, 2012; Li Piani, Weerheijm, Koene, et al., 2019). Furthermore,

despite significant advancements related to the use of Artificial Intelligence (AI), long simulation times limit their use for design purposes especially against highly dynamic loadings (Rocha et al., 2020). Therefore, analytical models are still widely used to gain fundamental insights into the physics governing material response for impact problems and to quickly infer estimations of fundamental parameters (Abrate, 2007; Li Piani et al., 2018). Among the class of analytical models, the so called phenomenological models derive functions for fundamental properties inherent dynamic loadings based on the parametrized assessment of the material response mechanisms (Iskander et al., 2015). Empirical models constitute the most straightforward approach. As an example, polynomial functions might be used to interpolate experimental force displacement response curves or out of plane panel profiles and relate these to applied ballistic impact (Caprino et al., 2007). These models are straightforward and simple to use; however they depend on the extension and consistency of the experimental dataset and need to be coupled with visual observations in order to gain insights on the corresponding failure mechanisms (Tsamasphyros & Bikakis, 2013). More recently, semi-empirical structural models have been developed. These parametrize the physics of the impact process by fitting material constants inherent to inertial, viscous and bearing strength terms based on Newtons' laws (Caprino et al., 2004). Within this class, the so called Energy Partition Method (EPM) has found extensive applications for the simulation of low and high velocity impact problems on composites (Hoo Fatt et al., 2003). The EPM constitutes an energy balance approach, which parametrizes the role of the different material constituents and of the key material properties by means of the equivalence between the energy input in the system and the corresponding sources of energy dissipations (Moriniere, 2014). During impact, a large variety of dissipation energy sources may arise for composite laminates: kinetic, elastic and plastic strain energy, fracture energy and even heat dissipation due to friction (Vlot, 1993). A reliable EPM must address all the individual sources of energy absorptions (Zhu & Chai, 2012). Contributions concern both inter ply failures e.g. delamination, and intra ply failures e.g. strength deterioration at the impacted side or matrix cracking and fibres cracking at the non-impacted surface (Hoo Fatt et al., 2003). These sources are included in many of these EPMs according to different theories of energy dissipations (Ouden, 2020). In this setting, plate or shell theories are often coupled with delamination theories and fracture models (Morinière, Alderliesten, Sadighi, et al., 2013). EPMs are usually implemented in a 2D domain; alternatively, equivalent mass-spring systems implementing dynamic equilibrium and conservation of energy equations are used (Tsamasphyros & Bikakis, 2013). An energy partition method was recently

developed at the Delft University of Technology to assess the ballistic performance of generic fibre metal laminates (Morinière, Alderliesten, & Benedictus, 2013). No applications of this method are available for blast loadings so far. In this research, this framework has been adopted to simulate the response of one TNO composite panel experimentally tested against blast loadings. In Section 2, the experimental reference used for the EPM simulation is provided. Next, the analytical framework of the energy partition method is explained. The actual code implementation developed at TNO to include blast loading case is detailed in Section 4 as well as it reports the main results from the EPM numerical simulation. Next, results are discussed against numerical simulations and experimental tests in literature.

2 Experimental reference

Between 2015 and 2019, TNO did research to develop a full composite concept which could outperform the aluminium and steel solutions against blast loadings. A TNO prototype was developed based on the theoretical hypothesis that early delamination in composites may trigger a shift from a bending to a preferred membrane behaviour. The mechanical properties of the TNO concept developed at TNO are reported in Table 1.

Table 1: List of parameters values (values have been scaled): density (ρ), length (L), height (H), thickness (b), Poisson's ratio (ν), elastic stiffness in fibre orientation and transverse (E), shear strength (S) and fracture shear energy (G). Mechanical properties are scaled by a scaling factor for confidentiality reasons.

ρ	L	H	b	ν	E_b	E_a	S	G
kg/m^3	m	m	m	[-]	Pa	Pa	Pa	kJ/m^2
2000	0.35	0.35	0.011	0.3	5E+9	2.0E+10	4.0E+07	5

Experimental tests on these full composite specimens were performed to assesses their response against blast loadings and compare it with standard aluminium. Blast tests were executed at TNO laboratories. These were executed using the ¼ scaled blast test setup developed at TNO. This type of testing was developed in 2015 as a quarter-scaled alternative to the full-scale STANAG 4569 (NATO AEP-55 STANAG 4569, 2010). In this setup, a thick steel box shaped support structure features a circular 340 mm diameter hole at the front, over which 600 x 600 mm panels can be positioned (Figure 1). Stereo cameras are placed inside the steel support structure in order to record the deformation of the panel

as it bulges inward. Digital image correlation system completes the installation. When detonated, the blast wave is supposed to push the panel inwards into the cut-out.

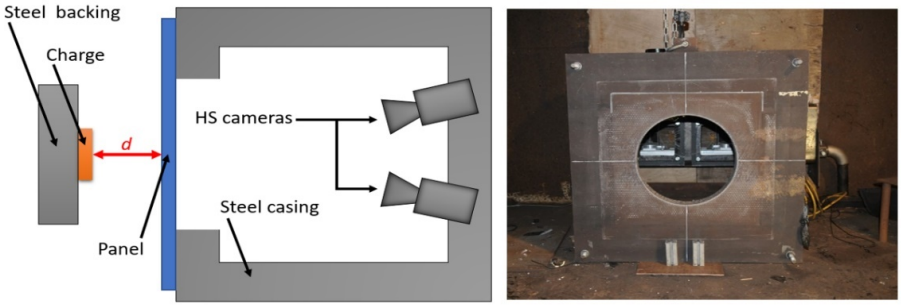

Figure 1: Schematic of the quarter-scale test setup (top view, left) and picture of the actual setup (front view, right)

Two different explosive charges were evaluated. The first charge was a 79 g explosive embedded in a so called steel pot. As an alternative configuration, a "puck charge" of 188 g was positioned directly on a steel backing plate as shown in Figure 1.

Comparisons with the experimental results of tests performed on full scale panels as well as FEM analyses assessed the scaled test method as suited for comparing different charge input (79 g steel pot and 188 g puck), stand-off distances (80 mm and 100 mm), materials options (11 mm and 15 mm thicknesses) and failure processes (Roebroeks, 2017a, 2017b). Out-of-plane displacement profiles of the horizontal mid-section of the tested panel were derived as a function of time by processing DIC sensors (Figure 2). Matlab code was implemented to calculate momentum, impulse, force as well as radius of curvature distributions along the panel as a function of time during loading. No empirical evidence of an early delamination inside the plies could be experimentally derived. However, in the early stages of blast to panel interaction, the measured strain levels using dic system in the panel back sides were found to be low in comparison with the corresponding strain values analytically calculated using the assumption that locally the material was in a pure bending mode.

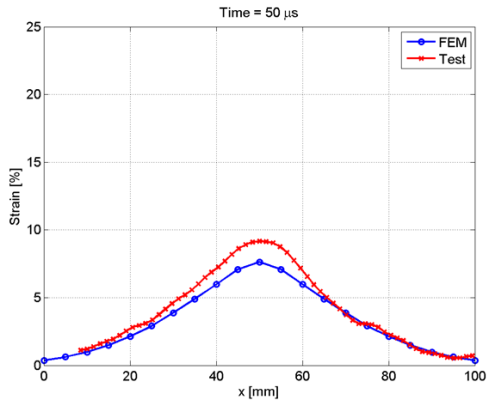

Figure 2: Scaled specimen installed in the support structure (lateral view, left), and example of experimental out-of-plane mid-section line displacement profiles comparison using FEM (right)

3 The Energy Partition Method on the blast response of composites

An energy partition method (EPM) has been implemented to simulate the blast response of the new composite concept developed at TNO. The EPM model developed at the Aerospace Faculty of Delft University of Technology has been adopted as an initial framework for this purpose (Moriniere, 2014). This has been implemented in a 1D setting (Figure 3).

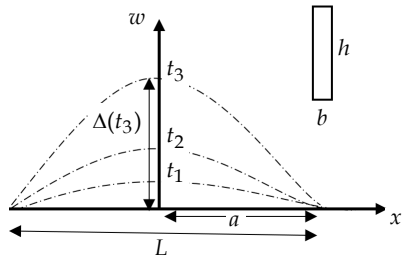

Figure 3: Top view of out-of-plane displacement profiles of mid-section panels as a function of time t (b, h: cross section thickness and height, a: panel half length, Δ: maximum transverse displacement)

The EPM starts its premises from the classical energy balance equation in Equation 1:

$$W_e = \Delta E_R \tag{1}$$

Where W_e is the external work and E_R collects the sources of energy dissipation related to all the resisting mechanisms activated during test. Provided an initial condition of static

rest (at time t_o = 0), the energy balance equation in (Morinière, Alderliesten, Sadighi, et al., 2013) reduces to Equation 2:

$$W_{e,kin}(t) = E_{fl}(t) + E_{del}(t) + E_{pet}(t) + E_{fr}(t) \tag{2}$$

where $W_{e,kin}$, E_{fl} , E_{del} , E_{pet} , E_{fr} are the kinetic, flexural, delamination, petaling and fracture energy terms respectively, calculated at a given time *t*. It is noteworthy that this quasi-static approach is rigorously valid only for closed systems (Hartle et al., 1995). $W_{e,kin}$ is the kinetic energy input in the system at *t*, calculated as in Equation 3:

$$W_{e,kin} = \frac{1}{2}\rho b A_e(t) V_e(t)^2 \tag{3}$$

where A_e is the cross section area of the portion of panel put in motion and V_e is the corresponding weighted mean velocity. A factor of 0.7 is used corresponding to velocity values along the panel lower than 60% of the peak velocity registered in the mid of the panel.

E_{fl} is the flexural energy absorbed by the induced out of plane displacement profile of the panel. According to both experimental evidence and numerical simulations from literature, a significant input energy is dissipated via composite bending during impact (Schipperen, 2019). In the hypothesis of pure elasticity, bending strain energy component is equal to:

$$E_{fl} = \frac{1}{2} E_b I \int_0^{L_{eq}} \chi^2(t) dx \tag{4}$$

Where E_b is the bending stiffness, *I* the moment of inertia of the panel, χ the panel curvature and L_{eq} is an equivalent length which calculates the portion of the panel put in motion. The stiffness of a plate determines its flexural behaviour (Morinière, Alderliesten, & Benedictus, 2013). Rigorously, the integral of the radius of curvature implies the assessment of the out-of-plane displacement profile of the laminate at each time step (Moriniere, 2014). During impact load, the flexural dissipation energy component may comprise both an elastic and inelastic regimes according to the induced displacement fields and strain rates. Therefore, stiffness degradation laws are necessary to assess the failure sequence during impact. According to the principles of continuum damage mechanics, the flexural energy term is thus generalized as it follows (Eq.5):

$$E_{fl} = \frac{1}{2} E_d I \int_0^{L_{eq}} \chi^2(t) dx \tag{5}$$

with:

$$E_d(t) = (1 - D(t)) E_b \tag{6}$$

where D defines the damage variable. This term comprises all sources of degradations which happen at a ply level, including matrix crushing, tensile cracking and fibre breaking. Its values range between 0 (in the elastic regime) and 1 (fully damaged material) and is activated if the elastic flexural energy exceeds the difference between the input energy and the remaining resisting components. The other possible failure modes reported in (Morinière, Alderliesten, Sadighi, et al., 2013) include delamination, backing material fracture and petaling as most significant contributors. Besides the deformation energy, only the delamination energy is considered in this paper. It is noted that other research also include friction and heat dissipations. In the current analysis all these energy terms have been neglected (Morinière, Alderliesten, & Benedictus, 2013).

E_{del} is the delamination energy. This term includes all the sources of energy dissipations inherent in inter-ply failure phenomena. The framework adopted from (Morinière, Alderliesten, Sadighi, et al., 2013) was in turn derived from the theory of delamination elaborated by Hoo Fatt for mid-span point load configurations (Hoo Fatt et al., 2003). Based on a greatly simplified shear stress distribution, this theory assumes a delamination propagation in mode II starting from a critical force F_y in equation 7:

$$F_y = \sqrt{\frac{8\pi^2 E_a b^3 G}{9(1 - \nu^2)}} \tag{7}$$

where ν is the laminate Poisson's ratio and G is the mode *II* critical interlaminar shear fracture toughness of the composite (Table 1). If the force input in the system is equal or higher than the threshold limit, delamination is activated and a radius of delamination R_0 is given by:

$$R_0 = \frac{F_y}{2\pi b S} \tag{8}$$

where S is the interlaminar shear strength. The corresponding energy can be calculated as in Equation 9:

$$E_{del} = \pi R_0^2 G \tag{9}$$

No petaling was experienced during blast load and the corresponding energy dissipation term has been ignored. Similarly, no steel plate was placed at the rear surface and thus fracture energy term was also neglected.

4 EPM model implementation and simulation results

It has been decided to simulate the blast response of one composite panel tested against blast loadings in Section 2. This panel will be named as 'Panel 1' in the following sections.

4.1 Kinetic Energy

As explained in Section 2, out-of-plane displacement, velocity and acceleration profiles over time for the panel mid-section have been made available by processing DIC sensor displacement histories in Matlab. Thus, all the terms inherent the kinetic energy can be directly implemented in Eq.3. It is noteworthy that the preliminary Eq. 2 is rigorously valid if the external work and the resisting energy terms in the balance equation at $t_0 = 0$ are null. A preliminary check was thus performed by extracting velocity and displacement profiles at the first time frame of measurement.

4.2 Flexure Energy

The integral of the curvature function of the composite panel over time is needed to derive the elastic flexure energy term in Equation 5. This implies the complete assessment of the out-of-plane displacement history function of the panel mid-section. In literature, several functions already exist to simulate the behaviour of the neutral axis of ballistically impacted composites (Moriniere, 2014). These equations are derived from analytical theories or fitted from experiments and are generally referred to specific impact regimes. The most commonly implemented stretching profiles for clamped panels centrally impacted are reported in Table 2 together with the corresponding impact regimes at which these were originally fitted (Eq. 10 a-c).

Besides experimental reference, the deflection field of a simply clamped plate can be also estimated from Timoshenko theory:

$$z = \Delta\left(1 - (\frac{x}{a})^2\right) \tag{11}$$

Table 2: Functions of the out-of-plane displacement profiles for centrally impacted panels

Reference	Regimes	Functions	
[20]	Ballistic	$z = \Delta\left(1 - \frac{2x}{a}\right)^2$	(10a)
[31]	Low and high velocity	$z = \Delta\left(1 + (\frac{x}{a})^2(\frac{2\ln x}{a} - 1)\right)$	(10b)
[32]	Quasi static to high velocity	$z = \Delta\left(1 + (\frac{x}{a})^2\right)^2\left(1 - 1.2\frac{x}{a} + 1.2(\frac{x}{a})^2\right)$	(10c)

Δ is the central transverse deflection and a is the span of the panel as in Figure 3.

It is worthy of note that this function may be used for moderately to thick plates, namely when the width to thickness ratio is lower than 50 (as valid for the application of this analysis); otherwise shear deformations are no longer negligible (Huang et al., 2008). A limitation to the straightforward use of these functions for the blast response assessment concern their regimes of applicability. In fact, the definition of a physically consistent displacement profile is key to develop an accurate flexural model: the precision of an energy balance model relies on the accurate estimation of the flexural displacement field that matches impact conditions. It is well known that target displacement profiles vary with impact regimes and may also shift from small to large deflections from static to high dynamic loadings (Baştürk et al., 2014). Therefore, functions implemented for high velocity impact may be not adequate in statics and vice versa. In addition, also for a given initial velocity, a multiplicity of strain rates may arise during impact history, thus potentially leading to shifts of displacement profiles as a function of time (Morinière, Alderliesten, Sadighi, et al., 2013). In absence of experimental data, also in (Morinière, Alderliesten, Sadighi, et al., 2013) a constant analytical function was implemented and variations in prediction accuracy of the force-time curves were observed over certain time intervals of the curve of response. Overall, the use of time independent functions is discouraged and transient profiles must be used. This hypothesis has been firstly experimentally validated. The experimental out-of-plane displacement history derived from DIC processed data on the tested panels described in Section 2 were compared with the existing analytical functions reported in Table 2. Results are showed for three panels. These are named as Panel 1, Panel 2 and Panel 3 in the following Table 3. Panel 2 has the same material and geometrical properties compared to Panel 1 but was loaded using a different charge typology. Panel 3 is thicker than Panel 1 but has been identically loaded. For all, the

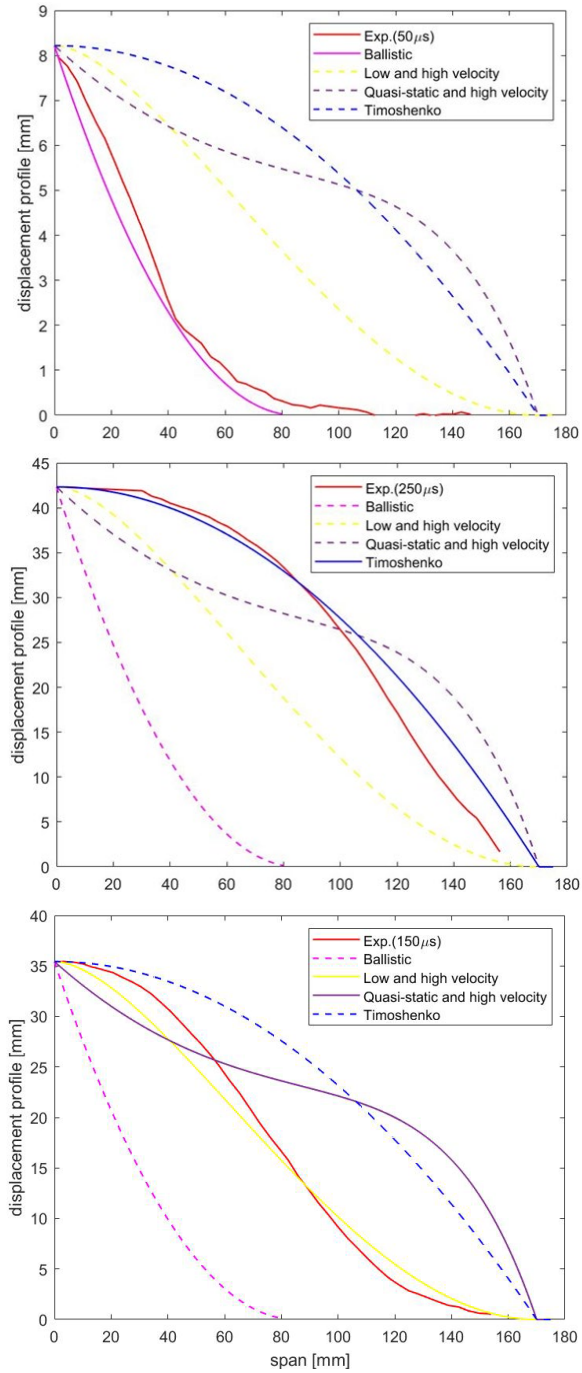

Figure 4: Experimental-analytical comparisons of mid span displacement profiles using formulations reported in Table 2 at different time steps (Panel 1)

experimental profiles at each available time step were compared with Equation 10a-10c. This comparison confirmed that analytical formulations developed to address the behaviour of panels at ballistic impact regimes (Eq. 10a) are prone to better address experiments at the earliest loading stages, when impulse is higher and induced strain rates are more localized around the centre of the panel (Fig. 4). On the contrary, Timoshenko formulations are better suited to fit the final stages of the panel response, when load has been transferred to the entire surface (Eq. 10c). At intermediate stages, formulations developed for a wide range of induced strain rates ranging from quasi statics to high velocity impact approximate the actual out-of-plane profiles (Fig. 4). The depicted trends are confirmed for all tests, independently from panel thickness and input charge (Fig. 5).

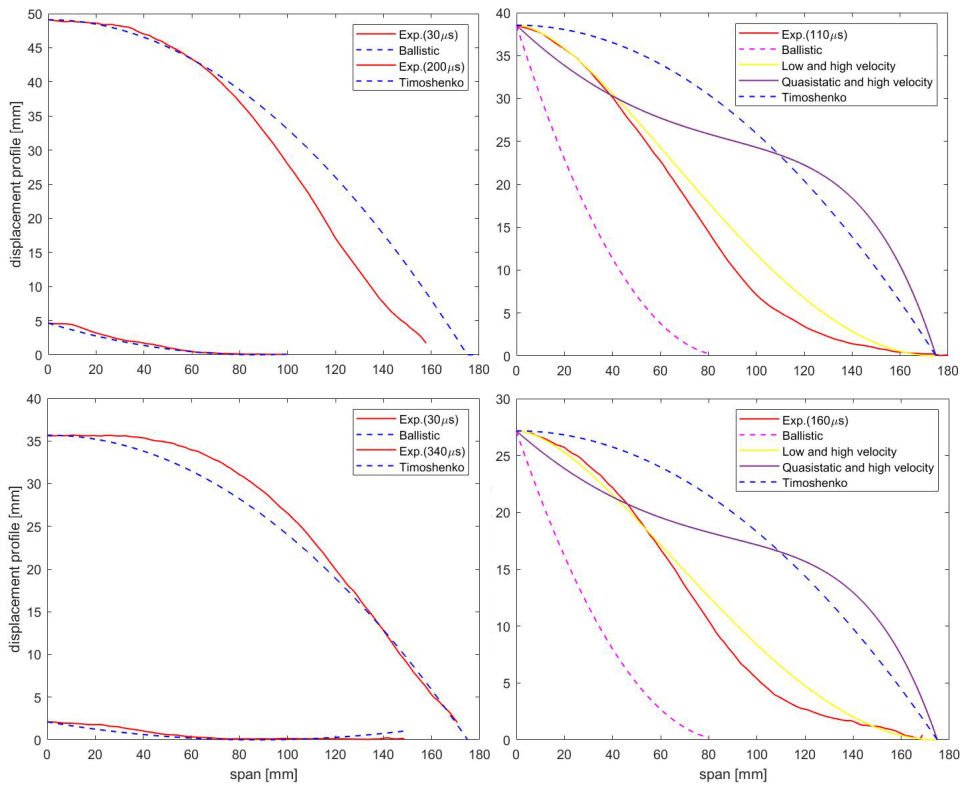

Figure 5: Experimental-analytical comparisons of mid span displacement profiles using formulations reported in Table 2 at different time steps (Panel 2, top and Panel 3, bottom)

Next, a transient analytical function is introduced to assess the out-of-plane response of composite laminates against blast loading. Consistently with main reference in literature, a simple second order polynomial function has been used in this work, in the form of Equation 12 (Morinière, Alderliesten, Sadighi, et al., 2013):

$$z(t) = a(t)x^2 + b(t)x + 1 \tag{12}$$

Time dependency in the equation is given by transient *a* and *b* parameters, which can be calibrated against experimental displacement. For each time step, normalized length-displacement curves have been fitted by a second order polynomial interpolation function in Matlab until 70% of the peak displacement decrease. For the tested panels, *a* and *b* values are listed in Table 3. The corresponding coefficients of determination are high for all

Table 3: Best fit parameters a and b for each time step t and corresponding values of maximum strain rates

Panel	t	$\dot{\varepsilon}_{max}$	r	a	b
	s	1/s	[-]	[-]	[-]
Panel 1	30	290	0.996	-3.7	-2.4
Panel 1	50	828	0.994	-3.3	-1.9
Panel 1	90	677	0.998	-2.4	-0.9
Panel 1	150	520	0.997	-2.2	-0.07
Panel 1	210	280	0.996	-1.5	-0.0009
Panel 1	250	262	0.98	-1.4	-0.0008
Panel 1	350	252	0.988	-1.1	0.24
Panel 2	60	1463	0.990	-3.8	-0.9
Panel 2	110	711	0.992	-1.8	-0.7
Panel 2	160	380	0.994	-1.5	-0.2
Panel 2	200	360	0.995	-1.4	0.2
Panel 2	240	358	0.992	-1.3	0.4
Panel 3	60	472	0.991	-6.1	-1.4
Panel 3	100	356	0.992	-2.9	-0.9
Panel 3	160	261	0.992	-2.1	-0.3
Panel 3	200	250	0.991	-1.5	-0.2
Panel 3	240	129	0.981	-1.4	-0.1
Panel 3	300	561	0.988	-0.7	0.04

tests and time steps (Fig. 6). Also in this case, the assessment is methodologically consistent for all the tested panels (Fig. 7).

The polynomial function and the corresponding *a* and *b* time histories for Panel 1 test have been implemented in the EPM. Once the displacement profiles were obtained, the curvature distribution history was automatically derived: The Newton's osculum was implemented in Matlab code (Gray, 1997). In the inelastic regime, an extra variable, the damage parameter D, must be implemented. In absence of experimental information on

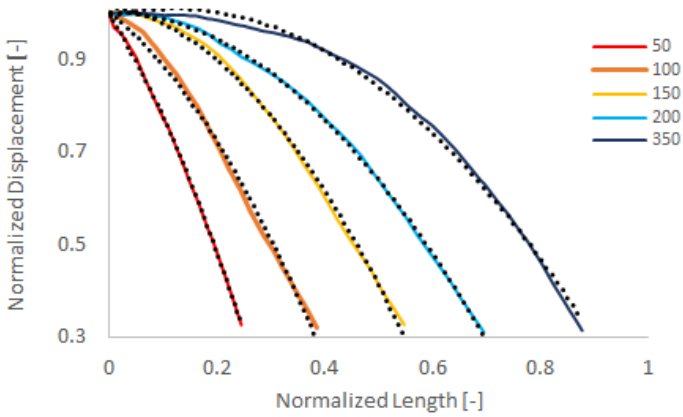

Figure 6: Experimental-analytical normalized profiles using a second order polynomial interpolation for different time steps on Panel 1(dotted lines: experiments; continuous line: model)

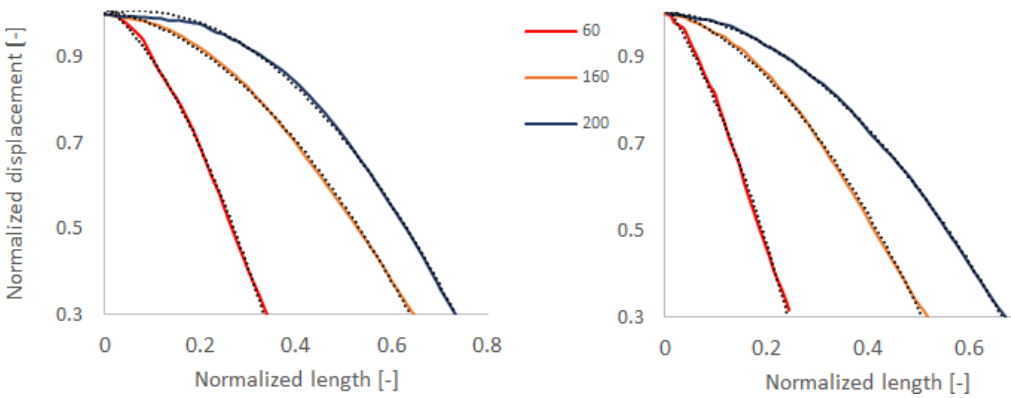

Figure 7: Experimental-analytical normalized profiles using a second order polynomial interpolation for different time steps on Panel 2 (left) and 3 (right)

the displacement evolution of the mid-section panel, in (Morinière, Alderliesten, & Benedictus, 2013) a time independent displacement model was coupled with a Tsai-Hill failure criterion in a 2D setting. Inherent failure parameters were tuned to match the overall force-displacement plot as experimentally derived. From tests at TNO, displacement and further time derivatives were made available. Thus, no predefined failure criterions were needed in a simplified 1D setting. Provided a closed form formulation for the delamination energy term, the actual damage evolution law could be derived by solving the energy balance equation at each time step.

*4.3 **Delamination energy***

At each time step, the delamination threshold force value has been checked against an equivalent point-load force. An equivalent force F_e acting on the system was obtained starting from the classical Newton's relation between impulse and momentum on weighted velocity profiles as in Equation 13:

$$\int_{t_0}^{t} F_e dt = \int_{t_0}^{t} M dv \tag{13}$$

where M is the mass of the panel. If the equivalent force was lower than the threshold limit, contribution of delamination was ignored. Else, delamination was active. The adopted theory by Hoo Fatt is a threshold energy criterion, namely the radius of delamination does not increase with time after delamination initiation (Hoo Fatt et al., 2003). However, this is considered to be not consistent with the physics observed in experiments for composite laminates (Caminero et al., 2017). Therefore, a delamination radius evolution law has been implemented in the model. No similar functions were available from literature. In absence of numerical or experimental information on the panel tested for simulation, an evolution law was implemented by analyzing the results of numerical simulations performed on previous experimental programs performed by the authors on two panels with different materials and geometries (Schipperen & Tang, 2019). For both, starting from normalized initiation times, average values for the radius R across the laminate were determined at each time step (Fig. 9).

Based on polynomial interpolation, an average evolution law has been implemented as representative of the case study of this simulation (Eq. 14):

$$\frac{R}{R_{0,d}} \sim 0.0006\,(\frac{t}{t_{0,d}})^3 - 0.03\,(\frac{t}{t_{0,d}})^2 + 0.5\frac{t}{t_{0,d}} + 0.6 \tag{14}$$

where $R_{0,d}$ is the radius at first time step, in which delamination is active (t_0, d).

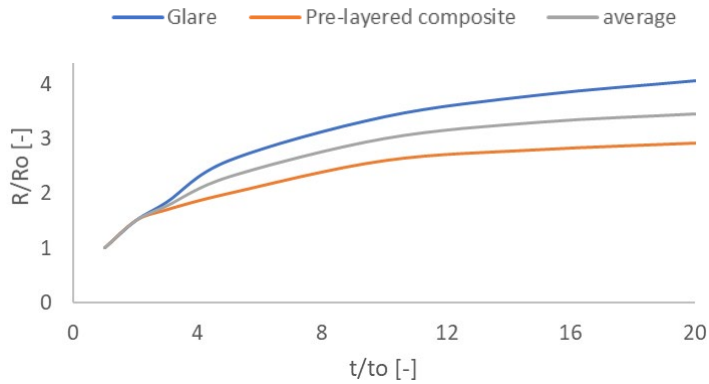

Figure 9: Delamination progressions from numerical simulations and average evolution law used in the current study

Table 4: Main results from model simulation: time t, kinetic energy E_{kin} , elastic bending energy Efl,e, Damage variable 1-D, radius of delamination R, delamination energy Ed and relative ratio with total energy

t	E_{kin}	$E_{fl,e}$	1-D	R	E_d	E_d / E_{kin}
ms	kJ	kJ	[-]	mm	J	%
30	19.9	20.1	1.0	26	64	0.32
50	91.9	85.2	1.0	31	81	0.11
90	76.3	173.7	0.44	39	135	0.20
110	66.5	181.5	0.37	43	175	0.26
130	60.1	210.6	0.29	47	209	0.34
150	42.4	181.0	0.23	52	241	0.65
210	15.8	88.5	0.16	58	330	1.9
250	10.1	64.8	0.15	62	370	3.5
310	8.9	75.0	0.12	65	441	4.3
410	3.3	42.5	0.07	71	495	8.8

4.4 Simulation results

Simulation results are collected in Table 4. Evolution in time of the kinetic energy in the system is also shown in Figure 10. The input energy ramps up to 92 kJ at 50 μs and progressively decays. Delamination starts before the peak and is detected since the first available time step of 30 μs in the analysis (Figure 10b). The relative contribution of delamination on the total absorbed energy is limited. Starting from 0.3% from the energy balance equation at 30 μs, it increases progressively up to about 5% for decreasing levels of energy in the system at late time steps (>300 μs). In contrast, the largest portion of the energy is absorbed through panel deformations. Until 50 μs, ply response appears to be elastic. After peak impulse, a positive damage variable emerges from EPM simulation (Figure 10c). Starting from a null value, damage parameter dramatically increases between 50 μs and 100 μs, anticipating a relatively smoother decaying branch for larger time steps.

5 Discussion of results

Results obtained from EPM are discussed in this section against literature findings and FEM results. Results from a FE analysis on the same panel were available (Schipperen, 2019). A literature review on the assessment of failure processes sequences on panels subjected to highly dynamic loadings was performed. In (Morinière, Alderliesten, Sadighi, et al., 2013), delamination in Glare panels subjected to ballistic impact occurred only at late stages of response. On the opposite, delamination is the first failure mode activated during dynamic impact for the full composite panels tested in this research (Figure 10). Also from FEM analysis, it was concluded that inter-ply delamination started between 15 μs and 35 μs after detonation, which is before the peak impulse was experienced by the panel, recorded between 40 μs and 50 μs. An average delamination radius of 54 mm through the laminate was extracted at around 50 μs (Figure 11). The relative modest contribution of delamination on the amount of energy directly dissipated is in agreement with experimental and numerical trends found in literature. Delamination energy in composites is generally found in a range between 2% and 12% of the total dissipated energy in literature (Sadighi et al., 2012) (Langdon et al., 2007). Peak values of delamination energies from simulation on the benchmark Panel 1 lie in this range (Table 4). Conversely, the largest amount of dissipated energy in the panel during blast load seems to result from out-of-plane deformations. Also from literature review, deformation energy usually accounts for up 80-90% of the total energy (Sadighi et al., 2012) (Langdon et al., 2007).

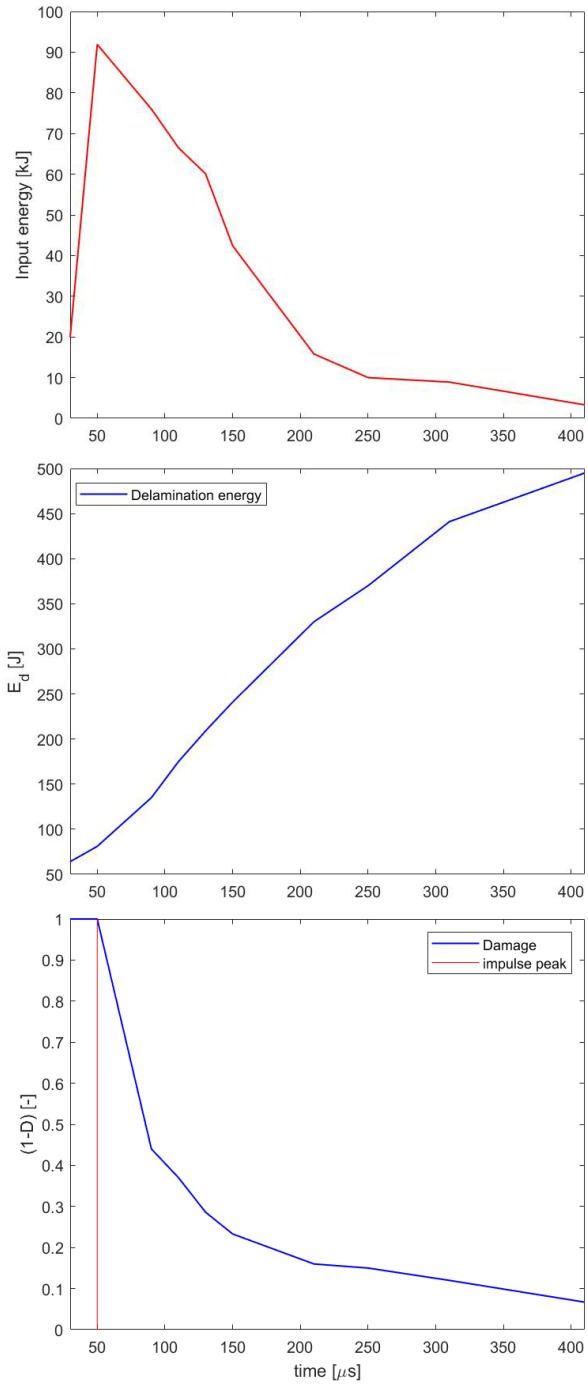

Figure 10: Time evolution of the input energy (top), delamination energy (middle) and damage (bottom) in the system

Furthermore, following delamination activation, the damage variable in the EPM model dramatically peaks to almost 0.6 between 50 μs and 100 μs (Figure 10). Also from FE simulation, plies were not found to suffer damage before peak impulse, whereas damage in plies was observed afterwards. Early delamination is used to interpret the physical meaning of the damage function in this EPM setting. In fact, visual observation reveals that the laminate is still providing significant bearing resistance in this interval (Figure 10). In this setting, the hypothesis of monolithicity is no longer valid and results into a much more stiff behaviour because delaminated plies start to respond individually, i.e. membrane action is activated. Thus, it is interpreted that the damage evolution law inherently includes a double contribution: an intra-ply material degradation caused by damage at the level of the matrix and fibre-matrix interfaces and a laminar structural degradation of the flexural response determined by a shift from pure bending to a preferred membrane response. This interpretation would explain the discrepancy observed between the actual bending strain values as extracted from DIC processed images and the elastic bending strains calculated via geometrical considerations ($\varepsilon = b\chi/2$), which is observed after 50 μs during simulation (Figure 11). Furthermore, this theory would also interpret the good blast response exhibited by the composite panels as a consequence of the preferred membrane stress built at initial stages of loadings and progressively stabilized at large time intervals, as shown in Figure 10. In fact, when only bending occurs, composites generally show limited resistance against blast loading. Their relatively high brittleness in comparison to metal cause an exceedance of strain to failure by local bending, fully absorbing the material straining capability, while the preferred membrane stress hardly develops. Composites more frequently tend to exhibit a bending profile, whereas metals a membrane-bending profile (Ursenbach et al., 1995). In this setting, delamination plays a fundamental role in brittle polymer composites and early delamination has the key function of triggering the loss of monolithicity and the resulting shift to a membrane behaviour (Zee & Hsieh, 1993). This interpretation is consistent with findings from e.g. (Hoo Fatt et al., 2003), where delamination was observed to reduce the panel bending stiffness and allowing higher transverse deformations to emanate away from impact location. Thus, a more likely mode of failure for laminated panels was concluded to be one involving large global deformations and tensile fracture rather than very much localized deformations. However, it is worthy of note that the structure of any analytical models is constrained by the material properties and the existence of failure modes are also directly linked to the impact regime (Hoo Fatt et al., 2003), (Vlot, 1993). The inclusion of a membrane component in Equation 1 aside flexure represents a next step forward for the EPM blast response model.

6 Conclusions

An energy partition method (EPM) recently developed at TU Delft to simulate the impact response of Glare Fibre Metal Laminate has been adapted to assess the behaviour of full composite panels subjected to blast loading. Flexural and delamination dissipation energy components were the two failure modes implemented in a 1D system of the panel. It is noteworthy that the reliability of this analytical approach can not overlook the assessment of the deformation fields of the panel, including its transient rate. Polynomial functions were defined in this research to interpolate the transient displacement fields of the panel. These are prone to represent an important improvement with respect to the use of constant displacement functions regardless type of analysis and loading rates. In addition, the inclusion of delamination evolution laws is necessary to infer physically consistent

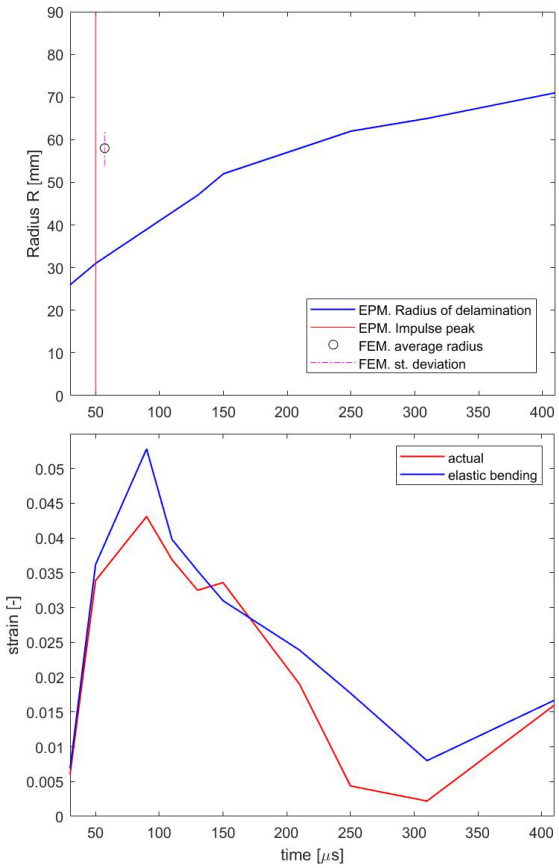

Figure 11: Analytical-numerical comparison between FEM and EPM radius of delamination (left), and analytical-experimental comparison of bending strain over time (right)

delamination processes. Both delamination evolution laws and displacement functions need experimental reference for interpolation similarly to experimental-numerical parameter fitting. Results from EPM simulation were confronted with equivalent information from FEM simulations on a blast test performed on a newly designed composite which outperforms aluminium. Comparison has revealed the suitability of a relatively simple analytical approach based on Newton's energy balance to address rough estimations of fundamental parameters, failure modes and sequences experienced by composite panels during blast loadings. For the designed composite, delamination starts before the panel experiences the peak impulse. However, its relative direct contribution to the total energy dissipated is modest. On the contrary, flexure governs the behaviour of the panel along the entire simulation. Damage in the ply laminate starts only after peak arise and dramatically ramps within a short time interval before it progressively smoothens. This trend can be interpreted as the effect of a double damage contribution, inherent material property degradation starting inside the matrix and/or fibre-matrix interfaces within the single ply and of an overall structural degradation of the panel monolithicity in the bending response. In this setting, besides its modest contribution, delamination plays a fundamental indirect role on the success of the blast performance of composite panels, by triggering the shift from pure bending to a preferred membrane behaviour responsible for governing the flexural response during blast load. The EPM could unveil this inner fundamental role, which cannot be recorded directly in experiments and comes at a high computational cost when numerical analyses are performed.

Literature

Abrate, S. (2007). Ballistic Impact on Composites. *16th International Conference on Composite Materials*, 1–10. https://doi.org/10.13140/2.1.2202.3044

Alderliesten, R. C., & Benedictus, R. (2008). Fiber/metal composite technology for future primary aircraft structures. *Journal of Aircraft*, 45(4), 1182–1189. https://doi.org/10.2514/1.33946

Allix, O. (2012). The bounded rate concept: A framework to deal with objective failure predictions in dynamic within a local constitutive model. *International Journal of Damage Mechanics*, 22(6), 808–828. https://doi.org/10.1177/1056789512468355

Baştürk, S., Uyanik, H., & Kazanci, Z. (2014). An analytical model for predicting the deflection of laminated basalt composite plates under dynamic loads. *Composite Structures*, 116(1), 273–285. https://doi.org/10.1016/j.compstruct.2014.05.018

Berhe, A. A. (2007). The contribution of landmines to land degradation. *Land Degradation & Development*, 18(1), 1–15. https://doi.org/10.1002/ldr.754

Caminero, M. A., García-Moreno, I., & Rodríguez, G. P. (2017). Damage resistance of carbon fibre reinforced epoxy laminates subjected to low velocity impact: Effects of laminate thickness and ply-stacking sequence. *Polymer Testing*, 63, 530–541. https://doi.org/10.1016/j.polymertesting.2017.09.016

Caprino, G., Lopresto, V., & Iaccarino, P. (2007). A simple mechanistic model to predict the macroscopic response of fibreglass-aluminium laminates under low-velocity impact. Composites Part A: *Applied Science and Manufacturing*, 38(2), 290–300. https://doi.org/10.1016/j.compositesa.2006.04.005

Caprino, G., Spataro, G., & Del Luongo, S. (2004). Low-velocity impact behaviour of fibreglass-aluminium laminates. Composites Part A: *Applied Science and Manufacturing*, 35(5), 605–616. https://doi.org/10.1016/j.compositesa.2003.11.003

Gray, A. (1997). Osculating Circles to Plane Curves. In CRC Press (Ed.), *Modern Differential Geometry of Curves and Surfaces with Mathematica*. CRC Press.

Hartle, J. B., Laflamme, R., & Marolf, D. (1995). Conservation laws in the quantum mechanics of closed systems. *Phys. Rev.* D, 51(12), 7007–7016. https://doi.org/10.1103/PhysRevD.51.7007

Hoo Fatt, M. S., Lin, C., Revilock, D. M., & Hopkins, D. A. (2003). Ballistic impact of GLARETM fiber-metal laminates. *Composite Structures*, 61(1–2), 73–88. https://doi.org/10.1016/S0263-8223(03)00036-9

Huang, Z. Y., Lü, C. F., & Chen, W. Q. (2008). Benchmark solutions for functionally graded thick plates resting on Winkler-Pasternak elastic foundations. *Composite Structures*, 85(2), 95–104. https://doi.org/10.1016/j.compstruct.2007.10.010

Iskander, M., Bless, S., & Omidvar, M. (2015). *Rapid penetration into granular media: Visualizing the fundamental physics of rapid earth penetration* (First). Elsevier Inc.

Langdon, G. S., Lemanski, S. L., Nurick, G. N., Simmons, M. C., Cantwell, W. J., & Schleyer, G. K. (2007). Behaviour of fibre-metal laminates subjected to localised blast loading: Part I-Experimental observations. *International Journal of Impact Engineering*, 34(7), 1202–1222. https://doi.org/10.1016/j.ijimpeng.2006.05.008

Li Piani, T., Weerheijm, J., Koene, L., & Sluys, L. J. (2019). The Adobe delta damage model: A locally regularized rate-dependent model for the static assessment of soil masonry bricks and mortar. *Engineering Fracture Mechanics*, 206(February), 114–130. https://doi.org/10.1016/j.engfracmech.2018.11.026

Li Piani, T., Weerheijm, J., & Sluys, L. J. (2018). Ballistic model for the prediction of penetration depth and residual velocity in adobe: A new interpretation of the ballistic resistance of earthen masonry. *Defence Technology*, 14(5), 4–8. https://doi.org/https://doi.org/10.1016/j.dt.2018.07.017

Li Piani, T., Weerheijm, J., & Sluys, L. J. (2019). Dynamic simulations of traditional masonry materials at different loading rates using an enriched damage delay: Theory and practical applications. *Engineering Fracture Mechanics*, 218(May). https://doi.org/10.1016/j.engfracmech.2019.106576

López-Puente, J., Zaera, R., & Navarro, C. (2007). An analytical model for high velocity impacts on thin cfrps woven laminates. *International Journal of Solids and Structures*, 44, 2837–2851.

Mohotti, D., Ngo, T., Raman, S. N., & Mendis, P. (2015). Analytical and numerical investigation of polyurea layered aluminium plates subjected to high velocity projectile impact. *Materials and Design*, 82, 1–17. https://doi.org/10.1016/j.matdes.2015.05.036

Moriniere, F. (2014). Low-velocity impact on fibre-metal laminates (Vol. 1, Issue 2012). Delft University of Technology.

Morinière, F. D., Alderliesten, R. C., & Benedictus, R. (2013). Low-velocity impact energy partition in GLARE. *Mechanics of Materials*, 66, 59–68. https://doi.org/10.1016/j.mechmat.2013.06.007

Morinière, F. D., Alderliesten, R. C., Sadighi, M., & Benedictus, R. (2013). An integrated study on the low-velocity impact response of the GLARE fibre-metal laminate. *Composite Structures*, 100, 89–103. https://doi.org/10.1016/j.compstruct.2012.12.016

NATO AEP-55 STANAG 4569. (2010).

Ouden, H. J. Den. (2020). Investigating Planar Delamination Behavior in Carbon Fiber Reinforced Polymer Panels An evaluation of delamination criteria Investigating Planar Delamination Behavior in Carbon Fiber Reinforced Polymer Panels An evaluation of delamination criteria. TU Delft.

Phu Nguyen, V., Lloberas Valls, O., Stroeven, M., & Johannes Sluys, L. (2010). On the existence of representative volumes for softening quasi-brittle materials - A failure zone averaging scheme. *Computer Methods in Applied Mechanics and Engineering*, 199(45–48), 3028–3038. https://doi.org/10.1016/j.cma.2010.06.018

Rocha, I. B. C. M., Kerfriden, P., & van der Meer, F. P. (2020). On-the-fly construction of surrogate constitutive models for concurrent multiscale mechanical analysis through probabilistic machine learning. 1–30. http://arxiv.org/abs/2007.07749

Roebroeks, G. e. al. (2017a). Development of a scaled vehicle underbelly blast test method. *25th International Symposium on Military Aspects of Blast and Shock*.

Roebroeks, G. et al. (2017b). Development of Fiber-Reinforced Composite Material for Blast Protection. *25th International Symposium on Military Aspects of Blast and Shock*, 5083.

Sadighi, M., Alderliesten, R. C., & Benedictus, R. (2012). Impact resistance of fiber-metal laminates: A review. *International Journal of Impact Engineering*, 49, 77–90. https://doi.org/10.1016/j.ijimpeng.2012.05.006

Schipperen, I. (2019). ERP Digital Twin Part C: Strip model to connect micro and meso-level composite blast panel simulations.

Schipperen, I., & Tang, L. (2019). Pretest Finite Element Analyses of composite flat panel and gull wing panels for testrig experiments - TNO report.

Tsamasphyros, G. J., & Bikakis, G. S. (2013). Analytical modeling to predict the low velocity impact response of circular GLARE fiber-metal laminates. *Aerospace Science and Technology*, 29(1), 28–36. https://doi.org/10.1016/j.ast.2013.01.005

Ursenbach, D. O., Vaziri, R., & Delfosse, D. (1995). An engineering model for deformation of CFRP plates during penetration. *Composite Structures*, 32(1–4), 197–202. https://doi.org/10.1016/0263-8223(95)00026-7

van der Meer, F. P., & Sluys, L. J. (2009). Continuum Models for the Analysis of Progressive Failure in Composite Laminates. *Journal of Composite Materials*, 43(20), 2131–2156. https://doi.org/10.1177/0021998309343054

Van der Meer, F., Sluys, L. J., Hallett, S., & Wisnom, M. (2012). Computational modeling of complex failure mechanisms in laminates. *Journal of Composite Materials*, 46(5), 603–623.

Vlot, A. (1993). Low-velocity impact loading: On fibre reinforced aluminium laminates (ARALL and GLARE) and other aircraft sheet materials. In Delft University of Technology, Faculty of Aerospace Engineering, Report LR-718. http://repository.tudelft.nl/islandora/object/uuid:9200a03f-00ab-4c90-8e38-20748dd5fde0?collection=research

Zee, R. H., & Hsieh, C. Y. (1993). Energy loss partitioning during ballistic impact of polymer composites. *Polymer Composites*, 14(3), 265–271. https://doi.org/10.1002/pc.750140312

Zhu, S., & Chai, G. B. (2012). Low-velocity impact response of fibre-metal laminates - Experimental and finite element analysis. *Composites Science and Technology*, 72(15), 1793–1802. https://doi.org/10.1016/j.compscitech.2012.07.016